Research Article

Blind Coarse Timing Offset Estimation for CP-OFDM and ZP-OFDM Transmission over Frequency Selective Channels

Vincent Le Nir (EURASIP Member),[1,2] **Toon van Waterschoot,**[1]
Jonathan Duplicy,[3] **and Marc Moonen (EURASIP Member)**[1]

[1] *Department of Electrical Engineering (ESAT/SISTA), Katholieke Universiteit Leuven, Kasteelpark Arenberg 10,*
  B-3001 Leuven-Heverlee, Belgium
[2] *Department of Communication Information Systems and Sensors (CISS), Royal Military Academy,*
  30 Avenue de la Renaissance, B-1000 Brussels, Belgium
[3] *Agilent Technologies Labs, WingePark 51, 3110 Rotselaar, Belgium*

Correspondence should be addressed to Vincent Le Nir, vincent.lenir@rma.ac.be

We present a blind coarse timing offset estimation technique for CP-OFDM and ZP-OFDM transmission over frequency selective channels. The technique exploits the cyclic prefix or zero-padding structure to estimate the starting position of the OFDM symbols without requiring any additional pilots. Simulation results are performed on various channel models with timing and frequency offsets. The presented technique is compared with the autocorrelation-based technique and various techniques in frequency selective channels. Our algorithm shows better performance results than those of the autocorrelation-based technique in NLOS channels, where the most predominant channel path is usually not the first arrival path.

1. Introduction

In this paper, we describe a technique to blindly estimate the timing offset in digital communications systems employing orthogonal frequency division multiplexing (OFDM). The starting position of the OFDM symbols is estimated using the cyclic prefix (CP) or zero-padding (ZP) structure of the transmitted signal without requiring any additional pilots. The aim of the paper is to provide an alternative coarse timing offset estimation technique to the autocorrelation-based technique [1–3] which does not perform well in non-line-of-sight (NLOS) frequency selective channels as well as for ZP-OFDM transmission.

The literature on timing offset estimation and carrier frequency offset (CFO) estimation can be divided in two categories: data-aided and non-data-aided techniques. Data-aided techniques use additional pilot symbols known at the receive side to estimate the timing and frequency offsets based on autocorrelation and other features [4–6]. Non-data-aided techniques do not require additional pilot symbols and can exploit the cyclic prefix structure of the transmitted signal in an autocorrelation metric [1, 3] (which is a simplified version of the maximum likelihood (ML) algorithm requiring the knowledge of the received signal-to-noise ratio (SNR) [2]). However, these techniques fail when the channel exhibits strong multipath components. Other non-data-aided techniques require the knowledge of the pulse shaping filter and exploit the cyclostationarity of the OFDM signal by a cyclic autocorrelation metric [7, 8], use bell-patterns to detect the symbol energy variations of the first subcarrier [9], require the knowledge of the maximum delay spread [10], or perform symbol timing and frequency offset estimation jointly [11].

In this paper, we propose a new non-data-aided approach for timing offset estimation which does not require the knowledge of the SNR [2], the pulse shaping filter [7, 8] or the maximum channel delay spread [10] and works well for CP-OFDM and ZP-OFDM transmission when the channel exhibits strong multipath components. For the mathematical derivations, we assume that the cyclic prefix duration T_{cp} or zero-padding duration T_{zp} is larger than the channel impulse response τ_{max}; however we will show that the algorithm still

exhibits good performance when $T_{cp} < \tau_{max}$ (or $T_{zp} < \tau_{max}$). Moreover, we assume the knowledge of the symbol duration T_u, the cyclic prefix duration T_{cp} (or the zero-padding duration T_{zp}) and the number of subcarriers N_c which can indeed be estimated blindly with the algorithms described in [12]. The timing offset estimation technique exploits the cyclic prefix or zero-padding structure of the OFDM signal and tracks time domain symbol energy variations based on a transition metric. Contrary to the autocorrelation metric [1–3], the transition metric-based technique is able to estimate the timing offset in frequency selective channels with strong multipath components.

The paper is organized as follows. In Section 2, we present the OFDM signal model, we review the technique for timing offset estimation based on the autocorrelation metric, and then the techniques based on the transition metric are presented for CP-OFDM and ZP-OFDM transmission. In Section 3, simulation results are presented with realistic channels models. Finally, conclusions are drawn in Section 4.

2. Description of the Algorithm

The non-data-aided technique presented in this paper has been developed in the context of radio surveillance and cognitive radio systems for multicarrier modulations. The wideband received signal may contain multiple OFDM signals of interest. Therefore, the received signal is sampled in a large bandwidth to include existing and future OFDM standards, such as Wifi (2.4 GHz or 5 GHz), WiMAX (3.5 GHz), Long-Term Evolution (LTE), or WiMedia (ECMA-368) signals. The carrier frequencies, bandwidths, and average powers of the detected signals are estimated. After downconversion to baseband and low-pass filtering, each signal of interest is processed through a feature detection block to determine whether or not it is an OFDM signal and to estimate blindly its symbol duration T_u, its cyclic prefix duration T_{cp} (or its zero-padding duration T_{zp}) and its number of subcarriers N_c [12]. Each signal of interest can be modeled as a received sequence $[y(0) \cdots y(N-1)]$ of length N such that

$$y(i) = e^{j(2\pi\epsilon i + \phi)} \sum_{\tau=\theta}^{\tau_{max}-1+\theta} h(\tau - \theta)x(i - \tau) + n(i),$$

(1)

$$i \in [0 \cdots N-1],$$

where $[x(0) \cdots x(N-1)]$ is the transmitted signal vector oversampled by the ratio between the cut-off frequency of the low-pass filter and the transmitter maximum frequency, the $h(\tau)$'s are the oversampled multipath channel coefficients with τ_{max} the number of channel taps, $[n(0) \cdots n(N-1)]$ is the vector of Additive White Gaussian Noise (AWGN), ϕ the receiver phase offset, ϵ the receiver frequency offset, and θ the receiver timing offset.

2.1. Timing Offset Estimation Techniques for CP-OFDM Transmission. The effect of the multipath replicas on the transmitted signal is shown on Figure 1. One can see that the multipath replicas reduce the number of samples in the cyclic prefix that are fully correlated to the samples in the last

part of the OFDM symbols (the number of samples being partially correlated increases, but the number of samples being fully correlated decreases). Assuming that the cyclic prefix length T_{cp} is larger than the channel impulse response τ_{max}, the length of the sequence showing such correlation is $T_{cp} - \tau_{max}$.

Knowing the symbol duration T_u and the cyclic prefix duration T_{cp}, the techniques in [1–3] propose to use an autocorrelation metric to estimate the timing offset. In this case, the timing offset estimate corresponds to the maximum of the correlation between the received sequence and the conjugated received sequence shifted by the symbol duration T_u over windows of length T_{cp}, as seen on Figure 2. The received sequence of length N is divided into M blocks of size $T_s = T_u + T_{cp}$ where the autocorrelation metric is performed on the available blocks except the last block. The autocorrelation metric is given by [3]

$$\theta_{opt} = \arg\max_{\theta} \frac{1}{(M-1)T_{cp}} \sum_{m=0}^{M-2} \left| \sum_{i=mT_s+T_u+\theta}^{(m+1)T_s+\theta-1} y(i)y^*(i - T_u) \right|.$$

(2)

However, maximizing the autocorrelation metric over a window of length T_{cp} will rather provide a timing offset estimate of the most predominant channel path than a timing offset estimate of the starting position for the OFDM symbols. Indeed, only a duration of $T_{cp} - \tau_{max}$ is fully correlated between the received sequence and the conjugated received sequence shifted by the symbol duration T_u. Therefore, the autocorrelation metric is expected to work well in line-of-sight (LOS) scenarios where the most predominant channel path is the first arrival path, but it will fail in NLOS scenarios where the most predominant channel path is usually not the first arrival path.

Instead of using an autocorrelation metric, we propose to use a metric-based on the difference between the received sequence and the same sequence shifted by the symbol duration T_u (see also Figure 2). The correlated duration $T_{cp} - \tau_{max}$ of the cyclic prefix is cancelled out in this operation. In this way, the cyclic prefix structure of the OFDM signal is exploited by tracking time domain symbol energy variations based on a transition metric between the end of the fully correlated duration $T_{cp} - \tau_{max}$ and the beginning of a new OFDM symbol. Contrary to the autocorrelation metric [2, 3], the transition metric-based technique is able to estimate the timing offset in frequency selective channels even with strong multipath components. The received sequence of length N is also divided into M blocks of size $T_s = T_u + T_{cp}$ where the transition metric is performed on the available blocks except the last block. The proposed transition metric is given by

$$\theta_{opt}$$

$$= \arg\max_{\theta} \left. \frac{\frac{1}{M-1} \sum_{m=0}^{M-2} |y(i+1) - y(i+1-T_u)|^2}{\frac{1}{M-1} \sum_{m=0}^{M-2} |y(i) - y(i-T_u)|^2} \right|_{i=(m+1)T_s+\theta-1}.$$
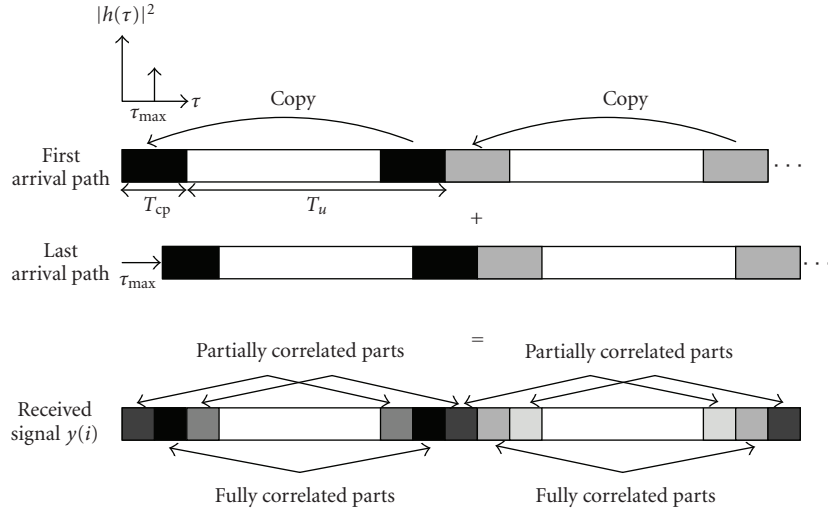
(3)

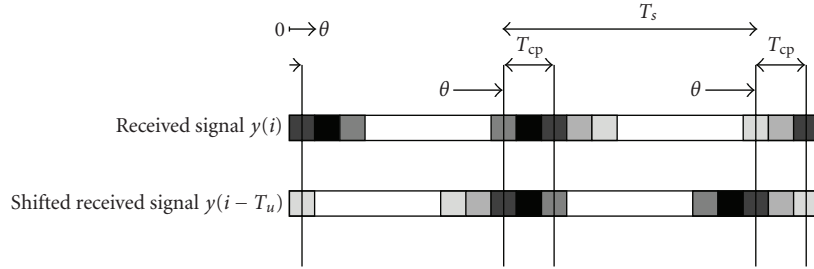FIGURE 1: Effect of the multipath replicas on the transmitted signal.

FIGURE 2: Windows used for timing offset estimation.

One can see that the modulus operation $|\cdot|$ is used outside the difference operation. This formula is especially suited for small CFOs. However, one can apply the modulus operation $|\cdot|$ to each component of the formula to make the algorithm insensitive to large CFOs. An algorithm that minimizes the difference metric between the received sequence and the same sequence shifted by the symbol duration T_u over a window duration N_p has been presented in [4]. The authors use prolonged guard intervals assuming a quite large ISI free period and known pilot symbols to provide fine-timing synchronization. In this paper, the ratio between two consecutive averaged difference metrics is calculated which require only one ISI free symbol to estimate the true timing offset (or even no ISI free symbol when $T_{cp} < \tau_{max}$ as long as the largest ratio index corresponds to the true timing offset). Moreover, it can be shown that averaging over several symbols in the same block has a negative impact on the timing offset estimate because this time smoothing will create an uncertainty on the starting position of the OFDM symbol [4].

The transition metric can be evaled for each index θ according to Figure 2 and ranging from $\theta = \tau_{max}$ to $\theta = T_s + \tau_{max}$. As the transition metric is the ratio between two consecutive averaged metrics, we define the difference metric $d(\theta) = E[|y(\theta) - y(\theta - T_u)|^2]$. When applying the signal model (1) to the difference metric (with $\epsilon = 0$), it can be shown that

$$d(\theta) = \begin{cases} 2\left(\sum_{\tau=0}^{\tau_{max}-1} |h(l)|^2 \sigma_x^2 + \sigma_n^2\right), & \tau_{max} \le \theta < T_u, \\ 2\left(\sum_{\tau=\theta-Tu+1}^{\tau_{max}-1} |h(l)|^2 \sigma_x^2 + \sigma_n^2\right), & T_u \le \theta < T_u + \tau_{max} - 1, \\ 2\sigma_n^2 & T_u + \tau_{max} - 1 \le \theta < T_s, \\ 2\left(\sum_{\tau=0}^{\theta-T_s} |h(l)|^2 \sigma_x^2 + \sigma_n^2\right), & T_s \le \theta < T_s + \tau_{max}. \end{cases} \tag{4}$$

The transition metric can be rewritten as

$$\theta_{opt} = \underset{\theta}{\operatorname{argmax}} \frac{d(\theta)}{d(\theta - 1)}. \tag{5}$$

The detection of the transition corresponding to (4) is given at delay $\theta = T_s$:

$$\frac{d(T_s)}{d(T_s - 1)} = \frac{|h(0)|^2 \sigma_x^2 + \sigma_n^2}{\sigma_n^2}, \tag{6}$$

while for other delays, the ratio can be considered very small especially at high SNR (ratio between two successive

elements of (4)). In the case $T_{cp} < \tau_{max}$, the detection of the transition is also given at delay $\theta = T_s$ by

$$\frac{d(T_s)}{d(T_s - 1)} = \frac{\sum_{\tau=T_{cp}+1}^{\tau_{max}-1} |h(l)|^2 \sigma_x^2 + |h(0)|^2 \sigma_x^2 + \sigma_n^2}{\sum_{\tau=T_{cp}}^{\tau_{max}-1} |h(l)|^2 \sigma_x^2 + \sigma_n^2}. \quad (7)$$

This proves that the proposed transition metric-based technique can exhibit good performance when $T_{cp} < \tau_{max}$ as long as the channel has smaller power components for delays larger than the cyclic prefix duration than the first tap (which can be considered valid for an exponentially decreasing power delay profile). For low SNR, the performance of the algorithm can be improved by considering multiple ratios K of the difference metric

$$\theta_{opt} = \underset{\theta}{argmax} \prod_{k=0}^{K} \frac{d(\theta + k)}{d(\theta - 1 - k)}. \quad (8)$$

The detection of the transition is also given at delay $\theta = T_s$. As K increases, the performance of the algorithm improves as long as the denominator falls in the correlated duration (ISI free part) $T_{cp} - \tau_{max}$.

2.2. Timing Offset Estimation Techniques for ZP-OFDM Transmission. A similar algorithm which tracks time domain symbol energy variations can be used for ZP-OFDM signals, where the autocorrelation metric also fails. We assume that the symbol duration T_s and the zero-padding duration T_{zp} have been estimated blindly according to the algorithm described in [12]. We also assume that the zero-padding duration T_{zp} is larger than the channel impulse response τ_{max}. In this case, the zero-padding structure of the received OFDM signal is exploited by tracking time domain symbol energy variations (transition metric) between the end of the duration $T_{zp} - \tau_{max}$ (noise only) and the beginning of a new OFDM symbol (the time domain symbol energy variations are not averaged over several symbols in the same block because this time smoothing has a negative impact on the timing offset estimate). The transition metric is performed on the available blocks except the last block and is given by

$$\theta_{opt} = \underset{\theta}{argmax} \left. \frac{(1/(M-1)) \sum_{m=0}^{M-2} |y(i+1)|^2}{(1/(M-1)) \sum_{m=0}^{M-2} |y(i)|^2} \right|_{i=(m+1)T_s+\theta-1}. \quad (9)$$

For ZP-OFDM signal, we define the difference metric $d(\theta) = E[|y(\theta)|^2]$. When applying the signal model (1) to the difference metric, it can also be shown that

$$d(\theta) = \begin{cases} \sum_{\tau=0}^{\tau_{max}-1} |h(l)|^2 \sigma_x^2 + \sigma_n^2, & \tau_{max} \leq \theta < T_u, \\ \sum_{\tau=\theta-T_u+1}^{\tau_{max}-1} |h(l)|^2 \sigma_x^2 + \sigma_n^2, & T_u \leq \theta < T_u + \tau_{max} - 1, \\ \sigma_n^2, & T_u + \tau_{max} - 1 \leq \theta < T_s, \\ \sum_{\tau=0}^{\theta-T_s} |h(l)|^2 \sigma_x^2 + \sigma_n^2, & T_s \leq \theta < T_s + \tau_{max}. \end{cases} \quad (10)$$

The transition metric and the detection value at delay $\theta = T_s$ are also given by (5), (6). For the case $T_{zp} < \tau_{max}$, the detection value at delay $\theta = T_s$ is given by (7). Multiple ratios of the difference metric can also be considered to improve the performance at low SNR. The performance of the algorithm improves as long as the denominator falls in the ISI free part $T_{zp} - \tau_{max}$. In the next section, simulation results compare the autocorrelation metric and the transition metric for CP-OFDM signals. For ZP-OFDM signals, the transition metric can also be compared to a correlation metric-based on a power mask in the time domain. Indeed, knowing the symbol duration T_s and the zero-padding duration T_{zp}, the power correlation metric finds the power mask p_θ of length T_s that maximize the correlation with the received power in the time domain. Assuming that the received power has been normalized to unity, the power correlation metric is given by

$$\theta_{opt} = \underset{\theta}{argmax} \frac{1}{MT_s} \sum_{m=0}^{M-1} \sum_{i=mT_s}^{(m+1)T_s-1} |y(i)|^2 p_\theta(i - mT_s) \quad (11)$$

with

$$p_\theta = \frac{1}{T_s - T_{zp}} \left[zeros(\theta), ones\left(T_s - T_{zp}\right), zeros\left(T_{zp} - \theta\right) \right]$$

$$\text{if } \theta < T_{zp},$$

$$p_\theta = \frac{1}{T_s - T_{zp}} \left[ones\left(\theta - T_{zp}\right), zeros\left(T_{zp}\right), ones(T_s - \theta) \right]$$

$$\text{if } \theta \geq T_{zp}. \quad (12)$$

3. Simulation Results

In this section, we evaluate the performance of the presented techniques for WiMAX [13] and WiMedia (ECMA-368) [14] signals on Stanford University Interim (SUI) [15] and IEEE 802.15.3a [16] channel models with various time and frequency offsets. Simulations' results are performed on 1000 Monte Carlo trials with 10 OFDM symbols. Two types of channels are chosen, the SUI-1 and the CM-1 channels which have LOS components for flat terrain with light tree density and the SUI-4 channel which has NLOS components for hilly terrain with heavy tree density. The different characteristics of SUI channels models are given in Table 1. For the CM channel models we refer to [16]. The parameters used for the WiMAX (CP-OFDM) and the WiMedia (ZP-OFDM) transmitters are given in Table 2. One can notice that $T_{zp} < \tau_{max}$ for the CM-1 channel.

Figure 3 shows the performance comparison between the autocorrelation metric [1, 3] and the transition metric-based techniques for CP-OFDM signals (WiMAX parameters) on SUI-1 and SUI-4 channel models with various timing and frequency offsets. Four other techniques are also included in this comparison, one being the minimum mean square error (MMSE) metric-based technique considering a summation length T_{cp} [4], two others being the MMSE and the maximum correlation (MC) metric-based techniques proposed

Table 1: SUI channel models.

SUI 1 channel			
	Tap 1	Tap 2	Tap 3
Delay (μs)	0	0.4	0.9
Power (dB)	0	-15	-20
K factor	4	0	0
Doppler (Hz)	0.4	0.3	0.5
SUI 4 channel			
	Tap 1	Tap 2	Tap 3
Delay (μs)	0	1.5	4
Power (dB)	0	-4	-8
K factor	0	0	0
Doppler (Hz)	0.2	0.15	0.25

Table 2: OFDM signal parameters.

Parameters	WiMAX	WiMedia
Bandwidth	10 MHz	528 MHz
N_c	256	128
Number of samples in $T_{cp,zp}$	64	37
T_u	25.6 μs	242.42 ns
$T_{cp,zp}$	6.4 μs	70.07 ns
Nb symbols	10	10
Channels	SUI-1&4	CM1
τ_{max}	0.9&4 μs	113.63 ns
Number of samples in τ_{max}	9&40	60

by [17] (MMSE1 and MC1) considering a summation length $T_{cp} + \tau_{max}$ (therefore requiring the knowledge of the channel delay spread τ_{max}), and the last one being the derivative metric-based technique proposed by [18]. The left figures plot the lock-in probability versus the SNR (the timing offset is simulated as an integer multiple of the receiver's sampling period). The lock-in probability is defined as the probability of finding the timing offset estimate falling in the ISI free region. Indeed, for CP-OFDM signals, some symbol timming error is tolerable as long as the receiver FFT window starts within the guard interval of the first arriving path that is not affected by the previous symbol due to the multipath channel [17]. The right figures plot the Coefficient Variation Root Mean Square Deviation CV(RMSD) for the timing offset parameter θ, which is defined as

$$\text{CV(RMSD)} = \frac{\sqrt{E\left[(\theta - \theta_{\text{true}})^2\right]}}{E[\theta]}. \quad (13)$$

The coefficient variation shows the dispersion of the timing offset parameter from its true value normalized to the mean of the observed value at a particular SNR threshold. One can see that the autocorrelation metric-based technique [1, 3] and the MMSE metric-based technique [4] give better results than the transition metric-based

technique for SUI-1 channels, with 3 dB difference at a lock-in probability of 0.8. As demonstrated in Section 3, for LOS channels the most predominant channel path is the first arrival path and the transition metric is averaged over 10 blocks while the autocorrelation metric is averaged over 10 blocks times the cyclic prefix duration. Although we have considered multiple ratios for the transition metric $K = 55$, the autocorrelation metric-based technique performs better than the transition metric-based technique owing to the exploitation of a larger number of symbols in the same OFDM block. Considering the knowledge of the channel delay spread τ_{max}, the performance of the MC1 and MMSE1 metric-based techniques [17] improves the SNR of the autocorrelation and MMSE metric-based techniques by 1 dB at a lock-in probability of 0.8. The derivative metric-based technique achieves the lowest SNR (-2 dB) at a lock-in probability of 0.8. However, the right figure shows that the derivative metric-based technique [18] gives the highest CV(RMSD) compared to the MC1 and MMSE1 metric-based techniques. The autocorrelation and MMSE metric-based techniques have lower CV(RMSD) than the derivative metric-based technique. The minimum CV(RMSD) is given by the transition based technique for SNR larger than 8 dB. For SUI-4 channels, the autocorrelation and MMSE metric-based techniques have similar performance compared to the transition metric-based technique for low SNRs. However, the transition metric-based technique gives significantly better results than the autocorrelation and MMSE metric-based techniques when the SNR is larger than 3 dB (we have considered multiple ratios for the transition metric $K = 24$). In fact, the autocorrelation and MMSE metric-based techniques cannot exceed a lock-in probability of 0.5 even at high SNR because the most predominant channel path is usually not the first arrival path. The MC1, MMSE1 (considering the knowledge of the channel delay spread τ_{max}), and derivative metric-based techniques achieve very good performance compared to the transition metric-based technique for SNRs lower than 13 dB. However, for higher SNRs, the transition metric-based technique outperforms the MC1, MMSE1, and derivative metric-based techniques which cannot exceed a lock-in probability of 0.8. The right figures show that the transition based technique gives closer estimates to the true value of the timing offset than the autocorrelation, MMSE, MC1, MMSE1, and derivative metric-based techniques at almost all SNR ranges for SUI-4 channels.

Figure 4 shows the performance comparison between the power correlation metric-based technique (knowing the symbol duration T_s and the zero-padding duration T_{zp}, the power correlation metric finds the power mask p_θ of length T_s that maximizes the correlation with the received power in the time domain) and the transition metric-based technique for ZP-OFDM signals (WiMAX parameters with the replacement of the cyclic prefix duration T_{cp} by the zero-padding duration T_{zp} on SUI-1 and SUI-4 channel models, and WiMedia ECMA-368 parameters on the CM-1 channel model) with various timing and frequency offsets. The left figures plot the lock-in probability versus the SNR. For ZP-OFDM signals, the probability of finding the

(a) SUI-1

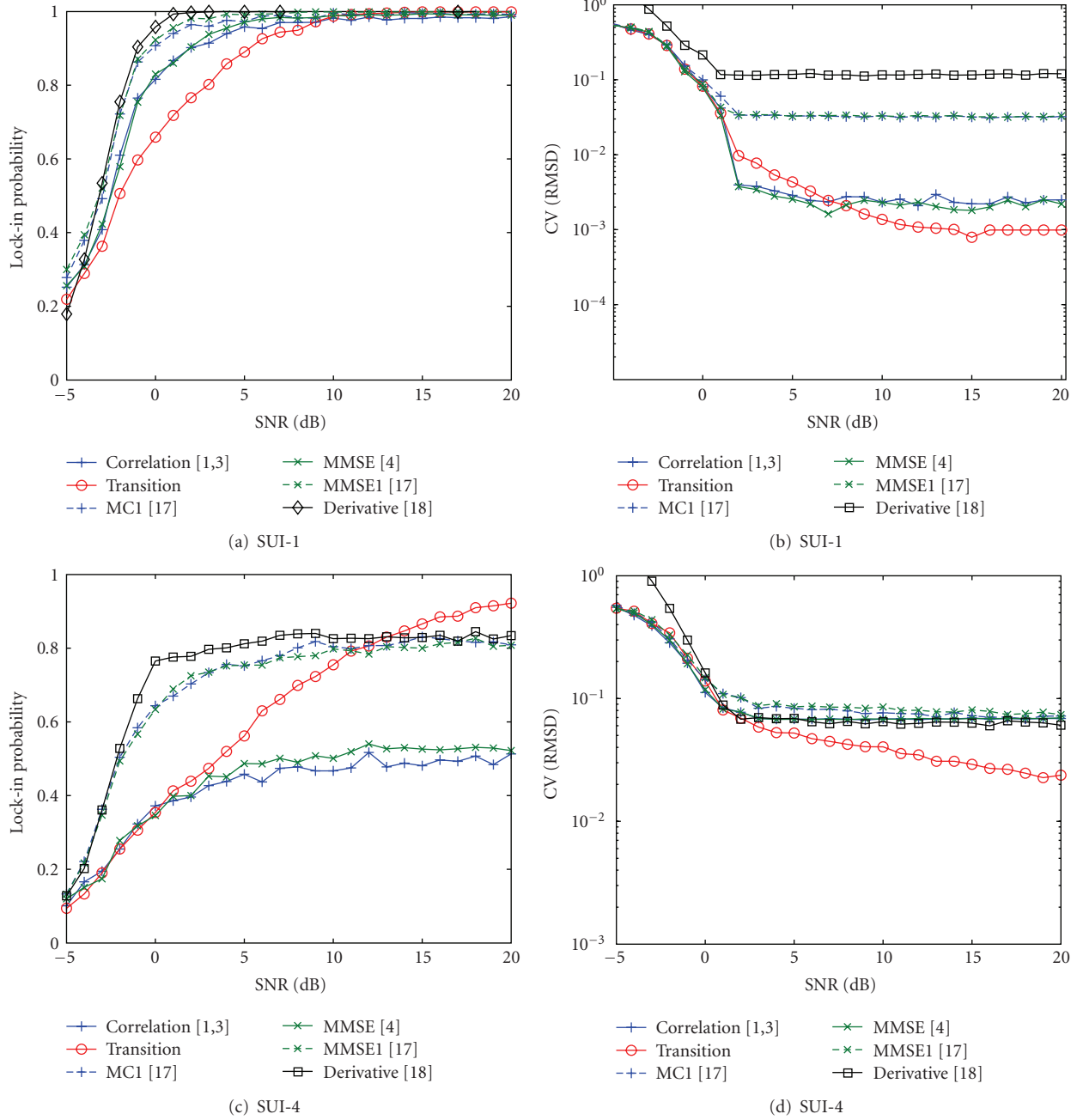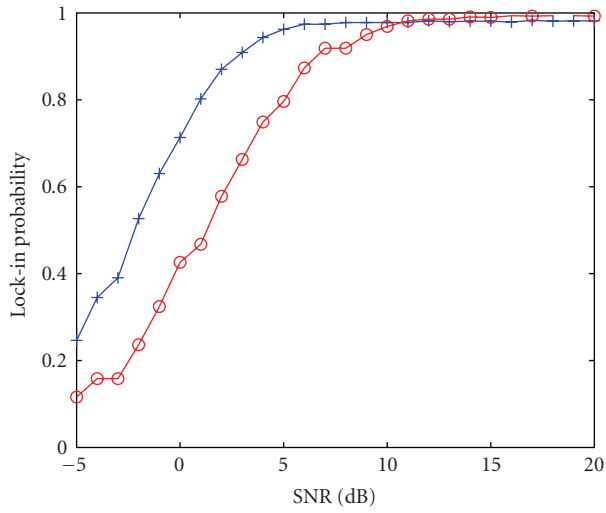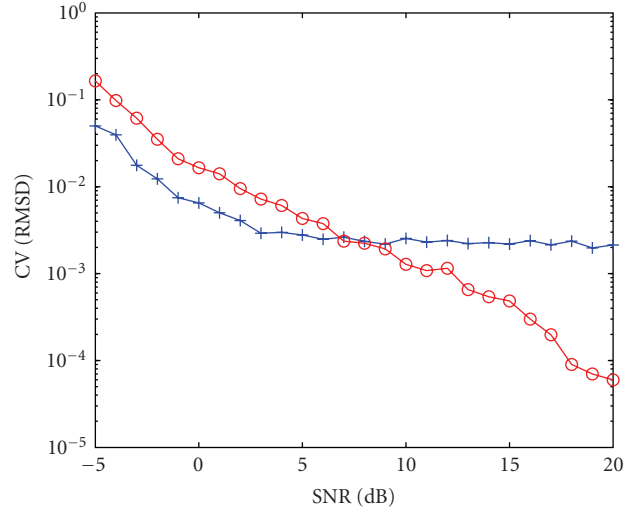(b) SUI-1

(c) SUI-4

(d) SUI-4

FIGURE 3: Simulations' results for CP-OFDM transmission.

timing offset estimate falling in the ISI free region is no longer valid. Therefore, the lock-in probability corresponds to the probability of finding the correct timing offset estimate θ_{true}. The right figures plot the CV(RMSD) for the timing offset parameter θ. For SUI-1 channels, the power correlation metric-based technique gives better results than the transition metric-based technique with 4 dB difference at lock-in probability of 0.8. As the transition metric is averaged over 10 blocks while the power correlation metric is averaged over 10 blocks times the symbol duration, the power correlation metric performs better than the transition

metric owing to the exploitation of a larger number of symbols in the same OFDM block (we have considered multiple ratios for the transition metric $K = 55$). The transition metric-based technique gives closer estimates to the true value of the timing offset when the SNR is larger than 8 dB. For SUI-4 channels, the transition metric-based technique gives better results than the power correlation metric-based technique when the SNR is larger than 5 dB (we have considered multiple ratios for the transition metric $K = 24$). One can see that the power correlation metric-based technique cannot exceed lock-in probability of 0.6 even
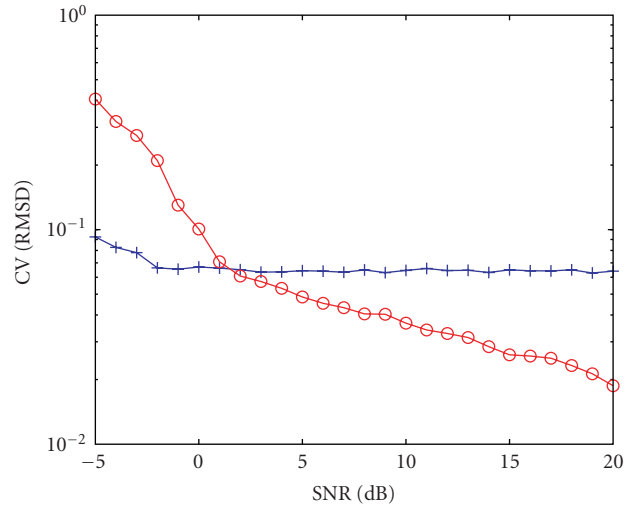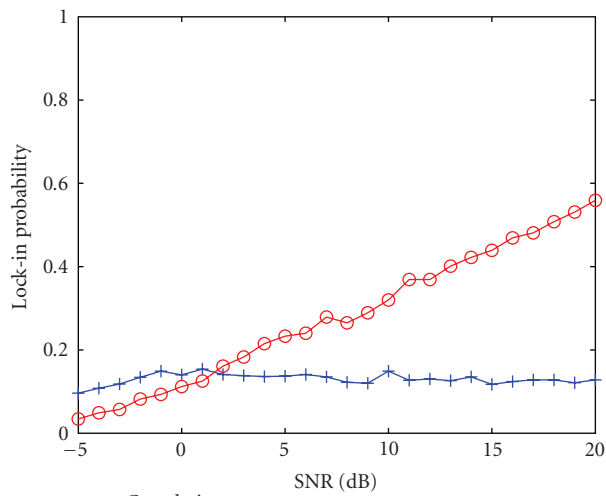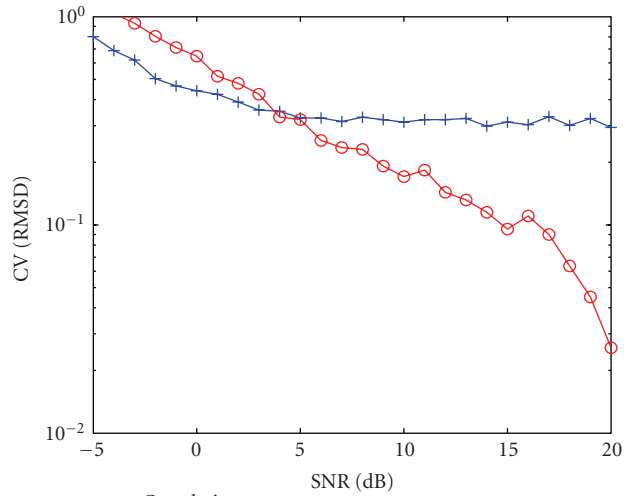
(a) SUI-1

(b) SUI-1
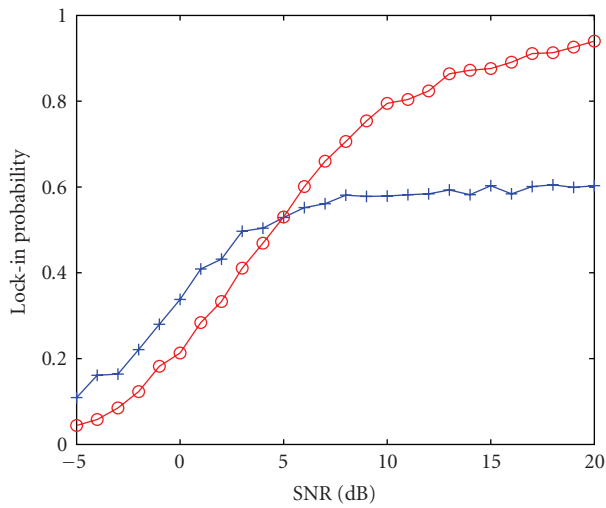
(c) SUI-4

(d) SUI-4

(e) CM-1

(f) CM-1

Figure 4: Simulations results for ZP-OFDM transmission.

at high SNR because the most predominant channel path is usually not the first arrival path. The transition metric-based technique gives closer estimates to the true value of the timing offset when the SNR is larger than 2 dB. For CM-1 channels, the transition metric-based technique consider multiple ratios $K = 10$. The power correlation metric-based technique cannot exceed lock-in probability of 0.1 even at high SNR because of the nature of the UWB channels (Saleh-Valenzuela) which produces multipath channels with different clusters. The transition metric-based technique gives higher lock-in probability than the power correlation based technique for SNR higher than 2 dB and gives closer estimates to the true value of the timing offset when the SNR is larger than 5 dB.

4. Conclusion

In this paper, we have described a technique to blindly estimate the timing offset in digital communications systems employing orthogonal frequency division multiplexing (OFDM). The starting position of the OFDM symbols has been estimated without any additional pilots using the cyclic prefix or zero-padding structure of the transmitted signal. This paper has provided an alternative coarse timing offset estimation technique to the autocorrelation-based technique which does not perform well in non-line-of-sight (NLOS) frequency selective channels as well as for ZP-OFDM transmission. The results confirm that the transition metric-based technique is able to estimate the timing offset in frequency selective channels with strong multipath components for CP-OFDM and ZP-OFDM transmission.

Acknowledgment

References

[1] T. Keller and L. Hanzo, "Orthogonal frequency division multiplex synchronisation techniques for wireless local area networks," in *Proceedings of the 7th IEEE International Symposium on Personal, Indoor and Mobile Radio Communications (PIMRC '96)*, vol. 3, pp. 963–967, Taipei, Taiwan, October 1996.

[2] J.-J. van de Beek, M. Sandell, and P. O. Börjesson, "ML estimation of time and frequency offset in OFDM systems," *IEEE Transactions on Signal Processing*, vol. 45, no. 7, pp. 1800–1805, 1997.

[3] M. Speth, S. Fechtel, G. Fock, and H. Meyr, "Optimum receiver design for OFDM-based broadband transmission—part II: a case study," *IEEE Transactions on Communications*, vol. 49, no. 4, pp. 571–578, 2001.

[4] M. Speth, F. Classen, and H. Meyr, "Frame synchronization of OFDM systems in frequency selective fading channels," in *Proceedings of the 47th IEEE Vehicular Technology Conference*, vol. 3, pp. 1807–1811, Phoenix, Ariz, USA, May 1997.

[5] T. M. Schmidl and D. C. Cox, "Robust frequency and timing synchronization for OFDM," *IEEE Transactions on Communications*, vol. 45, no. 12, pp. 1613–1621, 1997.

[6] H. Minn, V. K. Bhargava, and K. B. Letaief, "A robust timing and frequency synchronization for OFDM systems," *IEEE Transactions on Wireless Communications*, vol. 2, no. 4, pp. 822–839, 2003.

[7] H. Bölcskei, "Blind estimation of symbol timing and carrier frequency offset in wireless OFDM systems," *IEEE Transactions on Communications*, vol. 49, no. 6, pp. 988–999, 2001.

[8] B. Park, H. Cheon, E. Ko, C. Kang, and D. Hong, "A blind OFDM synchronization algorithm based on cyclic correlation," *IEEE Signal Processing Letters*, vol. 11, no. 2, part 1, pp. 83–85, 2004.

[9] A. J. Al-Dweik, "A novel non-data-aided symbol timing recovery technique for OFDM systems," *IEEE Transactions on Communications*, vol. 54, no. 1, pp. 37–40, 2006.

[10] R. Mo, Y. H. Chew, T. T. Tjhung, and C. C. Ko, "A new blind joint timing and frequency offset estimator for OFDM systems over multipath fading channels," *IEEE Transactions on Vehicular Technology*, vol. 57, no. 5, pp. 2947–2957, 2008.

[11] T. Fusco and M. Tanda, "ML-based symbol timing and frequency offset estimation for OFDM systems with noncircular transmissions," *IEEE Transactions on Signal Processing*, vol. 54, no. 9, pp. 3527–3541, 2006.

[12] V. Le Nir, T. Van Waterschoot, M. Moonen, and J. Duplicy, "Blind CP-OFDM and ZP-OFDM parameter estimation in frequency selective channels," *Eurasip Journal on Wireless Communications and Networking*, vol. 2009, Article ID 315765, 10 pages, 2009.

[13] 802.16e-2005, "Air interface for fixed and mobile broadband wireless access systemsAmendment for physical and medium access control layers for combined fixed and mobile operation in licensed band," 2005, *IEEE Standard*.

[14] Standard ECMA-368, "High Rate Ultra Wideband PHY and MAC standard," 2007, http://www.ecma-international.org/publications/files/ECMA-ST/ECMA-368 .pdf.

[15] IEEE 802.16 Broadband Wireless Access Working Group, "Channel models for fixed wireless application," 2003, *IEEE 802.16a-03/01*.

[16] J. Foerster, "IEEE 802.15.3a Channel modelling subcommittee," Report Final IEEE P802.15 Working Group for WPAN, 2002.

[17] D. Lee and K. Cheun, "Coarse symbol synchronization algorithms for OFDM systems in multipath channels," *IEEE Communications Letters*, vol. 6, no. 10, pp. 446–448, 2002.

[18] C. Williams, S. McLaughlin, and M. A. Beach, "Robust OFDM timing synchronisation in multipath channels," *Eurasip Journal on Wireless Communications and Networking*, vol. 2008, Article ID 675048, 12 pages, 2008.